



## Vibration Analysis of Circular Magneto-electro-elastic Nano-plates based on Eringen's Nonlocal Theory

A. Amiri\*, S. M. Fakhari, I. J. Pournaki, G. Rezazadeh, R. Shabani

Department of Mechanical Engineering, Urmia University, Urmia, Iran

### PAPER INFO

#### Paper history:

Received 16 October 2015

Received in revised form 15 November 2015

Accepted 24 December 2015

#### Keywords:

Magneto-electro-elastic

Nano-plates

Kirchhoff's Plate Theory

Nonlocal Elasticity

Natural Frequency

### ABSTRACT

The present work mainly studies the free vibration of circular magneto-electro-elastic (MEE) nano-plates based on Kirchhoff's plate theory within the framework of nonlocal elasticity theory to account for the small scale effect. The MEE nano-plate studied here is considered to be fully clamped and subjected to the external magnetic and electric potentials. Using nonlocal constitutive relations of MEE materials, the governing equations are derived by applying Maxwell's equation and Hamilton's principle. By employing Galerkin method, the eigen matrix form of the governing equation is obtained. The effect of magneto-electric potential on instability of the system is investigated and consequently critical values of applied potentials are calculated. A detailed numerical study is conducted to study the influences of the small scale effect, thickness and radius of the nano-plate and piezoelectric volume fraction of the MEE material on the natural frequencies of nano-plate. Furthermore, the effects of the applied magnetic and electric potentials on the size-dependent natural frequencies are investigated numerically.

doi: 10.5829/idosi.ije.2015.28.12c.15

### NOMENCLATURE

$c$	Elastic constant (GPa)	$e_0 a$	Nonlocal parameter
$e$	Piezoelectric constant (C/m <sup>2</sup> )	<b>Greek Symbols</b>	
$f$	Piezomagnetic constant (N/Am)	$\varepsilon$	Normal strain component
$k$	Dielectric constant (C/Vm)	$\gamma$	Shear strain component
$d$	Magneto electric constant (Ns/VC)	$\sigma$	Normal stress component
$D$	Electric displacement	$\mu$	Magnetic permeability (Ns <sup>2</sup> /C <sup>2</sup> )
$E$	Electric field	$\phi$	Electric potential
$B$	Magnetic induction	$\varphi$	Magnetic potential
$H$	Magnetic field	$\rho$	Mass density (Kg/m <sup>3</sup> )
$h$	Nano-plate thickness	$\nabla^2$	Laplacian operator
$R$	Nano-plate radius		

## 1. INTRODUCTION

In recent years, nano-scale structural elements such as nano-beams, nano-membranes, nano-plates, nanotubes and so others have attracted a great deal of attention.

Such nano-structures are used in different fields of nano-technology including nano-sensors, nano-oscillators, nano-actuators and nano-composites. It should be pointed out that nano-structures play an important role in nano-electromechanical (NEM) systems [1-5]. Due to the fact that the classical continuum elasticity is scale-independent theory, it may give inaccurate results in the analysis of nano-scale

\* Corresponding Author's Email: [ahadamiri69@yahoo.com](mailto:ahadamiri69@yahoo.com) (A. Amiri)

structures. In such structures, in order to predict an accurate behavior of them, small-scale effects should be taken into account. Various types of size-dependent theories such as couple stress theory, strain gradient theory and nonlocal elasticity theory have been developed by researchers in order to modify the classical continuum theory. Among all of these scale-dependent theories, the nonlocal elasticity theory developed by Eringen, has been used most commonly for analyzing mechanical behavior of nano-scale structures with good accuracy [6-9].

Because of their intrinsic coupling effects and adaptive properties, smart engineering structures constructed from the intelligent materials playing an important role in different fields of science such as nanotechnology. The MEE materials are a class of new smart materials which have attracted much attention of investigators in recent years. Due to the fact that the MEE materials are made from both piezoelectric and piezomagnetic phases, their mechanical properties can be affected by applying magnetic and electric potentials. In the other words, they can exhibit three phase coupling effects between magnetic, electric and mechanical fields. Therefore, they are able to convert energy among magnetic, electric and mechanical energies to each other. Compared with the single phase smart materials such as piezoelectric and piezomagnetic, the MEE composite materials include new properties of magneto-electricity with secondary pyro-electric effects. These properties allow them to be more sensitive and adaptive. It is worth mentioning that the obtained magneto-electric effects of MEE composite materials will be hundred times larger than that of a single phase piezoelectric or piezomagnetic material. These new properties can be useful to design more efficient sensors and actuators used in the smart or intelligent structures [10-15].

To date, some works have been done to study the mechanical behavior of MEE plates. Using Mindlin theory, Li [16] investigated buckling of MEE plate resting on Pasternak elastic foundation. Alaimo et al. [17] presented an isoparametric four-node finite element method for multilayered MEE plates. Equivalent single-layer plate theory was employed in their study considering quasi-static behavior of electric and magnetic fields based on first order shear deformation theory. Free and deterministic vibrations of a fluid-contacting isotropic MEE rectangular plate were investigated by Chang [18]. Liu [19] obtained closed form expressions for bending of MEE rectangular plates. Furthermore, they presented exact solutions for deformation behavior of BaTiO<sub>3</sub>-CoFe<sub>2</sub>O<sub>4</sub> MEE composites. Using the von Karman plate theory, Xue et al. [20] investigated large deflection of a rectangular MEE thin plate. In their work, Bubnov-Galerkin method was used for transforming the obtained nonlinear

equation to a third-order algebraic equation. Li et al. [21] studied buckling and free vibration of MEE rectangular nanoplate based on the nonlocal theory, considering Mindlin plate theory. In their analysis, effects of magneto-electric potential, spring and shear coefficients of Pasternak foundation on buckling load were investigated.

To date, no literature has been reported for the detailed study of vibration characteristics of MEE circular nano-plates model incorporating the size effect which become more significant and must be considered for thin nano-plates. To the authors best knowledge, this is the first attempt on the free vibration analysis of circular MEE nano-plates based on the Kirchhoff's plate theory considering nonlocal elasticity theory. Employing Hamilton's principle, governing equations are obtained and, subsequently, to obtain the natural frequencies, eigen matrix form of the equation is solved. Numerical results reveal the effects of the nonlocal parameter, thickness, radius and external magneto-electric potential on the size-dependent natural frequencies. Moreover, the effect of piezoelectric volume fraction percentage on vibration and natural frequency is determined and results are considered to highlight the behavioral difference of classic nanoplates with nonclassical ones.

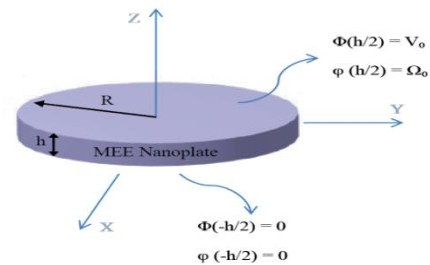


**Figure 1.** MEE circular nano-plate under magneto-electric loading.

## 2. NONLOCAL MEE NANO-PLATE MODEL

According to Kirchhoff's plate theory, the displacement field in cylindrical coordinates is expressed as follows:

$$\begin{aligned} u_r(r, \theta, z, t) &= -z \frac{\partial w(r, \theta, t)}{\partial r}, u_\theta(r, \theta, z, t) = \\ &= -z \frac{\partial w(r, \theta, t)}{r \partial \theta}, u_z(r, \theta, z, t) = w(r, \theta, t) \end{aligned} \quad (1)$$

where,  $u_r$ ,  $u_\theta$  and  $u_z$  are displacement components in radial, circumferential and transversal directions of the micro diaphragm, respectively (see Figure 1). Using the displacement components and neglecting the normal

strain in the thickness direction of the plate, the strains can be written as:

$$\begin{aligned} \varepsilon_r &= -z \frac{\partial^2 w}{\partial r^2}, \varepsilon_\theta = -z \left( \frac{1}{r} \frac{\partial w}{\partial r} + \frac{1}{r^2} \frac{\partial^2 w}{\partial \theta^2} \right), \\ \gamma_{r\theta} &= -2z \frac{\partial}{\partial r} \left( \frac{1}{r} \frac{\partial w}{\partial \theta} \right) \end{aligned} \quad (2)$$

Due to axisymmetric deflection of the circular plates, the strains expressed in Equation (2) can be denoted as following:

$$\varepsilon_r = -z \frac{\partial^2 w}{\partial r^2}, \varepsilon_\theta = -z \frac{1}{r} \frac{\partial w}{\partial r}, \gamma_{r\theta} = 0. \quad (3)$$

For a circular MEE plate structure, the nonlocal constitutive relations are given as [22, 23]:

$$(1 - (e_0 a)^2 \nabla^2) \sigma_r = c_{11} \varepsilon_r + c_{12} \varepsilon_\theta + c_{13} \varepsilon_z - e_{31} E_z - f_{31} H_z \quad (4)$$

$$(1 - (e_0 a)^2 \nabla^2) \sigma_\theta = c_{12} \varepsilon_r + c_{11} \varepsilon_\theta + c_{13} \varepsilon_z - e_{31} E_z - f_{31} H_z \quad (5)$$

$$(1 - (e_0 a)^2 \nabla^2) D_z = e_{31} \varepsilon_r + e_{31} \varepsilon_\theta + e_{33} \varepsilon_z + k_{33} E_z + d_{33} H_z \quad (6)$$

$$(1 - (e_0 a)^2 \nabla^2) B_z = f_{31} \varepsilon_r + f_{31} \varepsilon_\theta + q_{33} \varepsilon_z + d_{33} E_z + \mu_{33} H_z \quad (7)$$

$$(1 - (e_0 a)^2 \nabla^2) D_r = e_{15} \gamma_{rz} + k_{11} E_r + d_{11} H_r \quad (8)$$

$$(1 - (e_0 a)^2 \nabla^2) B_r = f_{15} \gamma_{rz} + d_{11} E_r + \mu_{11} H_r \quad (9)$$

$$(1 - (e_0 a)^2 \nabla^2) D_\theta = e_{15} \gamma_{\theta z} + k_{11} E_\theta + d_{11} H_\theta \quad (10)$$

$$(1 - (e_0 a)^2 \nabla^2) B_\theta = f_{15} \gamma_{\theta z} + d_{11} E_\theta + \mu_{11} H_\theta \quad (11)$$

where,  $e_0 a$  is specified as the parameter showing the small scale effect on the response of the structure and may be determined from experiments or by matching dispersion curves of plane waves with those of atomic lattice [24]. The strain energy of the system is written as:

$$U_e = \frac{1}{2} \int_V (\sigma_r \varepsilon_r + \sigma_\theta \varepsilon_\theta + \sigma_{r\theta} \gamma_{r\theta} - D_z E_z - B_z H_z - D_r E_r - B_r H_r - D_\theta E_\theta - B_\theta H_\theta) dV \quad (12)$$

According to Maxwell's equation, the electric and magnetic fields can be expressed as:

$$E_z = -\frac{\partial \phi}{\partial z}, H_z = -\frac{\partial \varphi}{\partial z} \quad (13)$$

Due to the fact that the nano-plate is thin, the in-plane magnetic and electric field is neglected and it is supposed that the nano-plate is polarized in the z direction. Therefore, substituting Equations (3) and (13) into Equation (12) leads to:

$$U_e = \frac{1}{2} \int_V \left\{ -\sigma_r z \frac{\partial^2 w}{\partial r^2} - \sigma_\theta z \frac{1}{r} \frac{\partial w}{\partial r} + D_z \frac{\partial \phi}{\partial z} + B_z \frac{\partial \varphi}{\partial z} \right\} dV \quad (14)$$

Bending moments are given by:

$$M_r = \int_{-h/2}^{h/2} \sigma_r z dz, M_\theta = \int_{-h/2}^{h/2} \sigma_\theta z dz \quad (15)$$

Considering Equation (15), the strain energy can be rewritten as:

$$\begin{aligned} U_e &= -\frac{1}{2} \int_A (M_r \frac{\partial^2 w}{\partial r^2} + M_\theta \frac{1}{r} \frac{\partial w}{\partial r}) dA + \\ &\frac{1}{2} \int_V (D_z \frac{\partial \phi}{\partial z} + B_z \frac{\partial \varphi}{\partial z}) dV \end{aligned} \quad (16)$$

The kinetic energy of the nano-plate because of its vibration can be expressed as follows:

$$U_T = \frac{1}{2} \int_A \rho h \left( \frac{\partial w}{\partial t} \right)^2 dA \quad (17)$$

The boundary conditions of the applied external electric and magnetic potentials are assumed to be as:

$$\phi(h/2) = V_0, \phi(-h/2) = 0 \quad (18)$$

$$\varphi(h/2) = \Omega_0, \varphi(-h/2) = 0 \quad (19)$$

The applied magnetic and electric potential can induce radial and circumferential loads which can be calculated from Equations (20) and (21) [16, 21].

$$N_r^e = N_r^\theta = e_{31} V_0 \quad (20)$$

$$N_m^r = N_m^\theta = f_{31} \Omega_0 \quad (21)$$

The external virtual work due to the magnetic and electric loads is described as:

$$\delta U_F = \int_A ((N_m^r + N_m^\theta) \left\{ \frac{\partial^2 w}{\partial r^2} + \frac{1}{r} \frac{\partial w}{\partial r} \right\}) \delta w dA \quad (22)$$

The Hamilton's principle is considered as follows:

$$\int_0^t (\delta U_T + \delta U_F - \delta U_e) dt = 0 \quad (23)$$

By employing Hamilton's principle, the following equations are resulted:

$$\begin{aligned} \frac{\partial^2 M_r}{\partial r^2} + \frac{2}{r} \frac{\partial M_r}{\partial r} - \frac{1}{r} \frac{\partial M_\theta}{\partial r} + \\ (N_m^r + N_m^\theta) \left\{ \frac{\partial^2 w}{\partial r^2} + \frac{1}{r} \frac{\partial w}{\partial r} \right\} - \rho h \frac{\partial^2 w}{\partial t^2} = 0 \end{aligned} \quad (24)$$

$$\frac{\partial}{\partial z} (D_z) = 0 \quad (25)$$

$$\frac{\partial}{\partial z} (B_z) = 0 \quad (26)$$

Satisfying Equations (25) and (26), one can obtain the following equations:

$$e_{31}\nabla^2 w + k_{33} \frac{\partial^2 \phi}{\partial z^2} + d_{33} \frac{\partial^2 \varphi}{\partial z^2} = 0 \tag{27}$$

$$f_{31}\nabla^2 w + d_{33} \frac{\partial^2 \phi}{\partial z^2} + \mu_{33} \frac{\partial^2 \varphi}{\partial z^2} = 0 \tag{28}$$

where,

$$\nabla^2 = \frac{\partial^2}{\partial r^2} + \frac{1}{r} \frac{\partial}{\partial r} \tag{29}$$

Solving Equations (27) and (28) leads to the following results:

$$\frac{\partial^2 \phi}{\partial z^2} = -M_1 \nabla^2 w, \quad \frac{\partial^2 \varphi}{\partial z^2} = -M_2 \nabla^2 w \tag{30}$$

in which,

$$M_1 = (e_{31}\mu_{33} - d_{33}f_{31}) / (k_{33}\mu_{33} - d_{33}^2) \tag{31}$$

$$M_2 = (k_{33}f_{31} - d_{33}e_{31}) / (k_{33}\mu_{33} - d_{33}^2) \tag{32}$$

Finally, solving Equation (30) results in:

$$\frac{\partial \phi}{\partial z} = -M_1 z \nabla^2 w + \phi_0 \tag{33}$$

$$\frac{\partial \varphi}{\partial z} = -M_2 z \nabla^2 w + \varphi_0 \tag{34}$$

Considering Equations (4) and (5), and using Equation (15) yields:

$$(1 - (e_0 a)^2 \nabla^2) M_r = -\tilde{c}_{11} \frac{h^3}{12} \frac{\partial^2 w}{\partial r^2} - \tilde{c}_{12} \frac{h^3}{12} \frac{1}{r} \frac{\partial w}{\partial r} \tag{35}$$

$$(1 - (e_0 a)^2 \nabla^2) M_\theta = -\tilde{c}_{12} \frac{h^3}{12} \frac{\partial^2 w}{\partial r^2} - \tilde{c}_{11} \frac{h^3}{12} \frac{1}{r} \frac{\partial w}{\partial r} \tag{36}$$

in which,

$$\tilde{c}_{11} = c_{11} + e_{31} M_1 + f_{31} M_2 \tag{37}$$

$$\tilde{c}_{12} = c_{12} + e_{31} M_1 + f_{31} M_2 \tag{38}$$

Substituting Equations (35) and (36) into Equation (24), the dynamic motion equation takes the following form:

$$\tilde{c}_{11} \frac{h^3}{12} \nabla^4 w - (1 - (e_0 a)^2 \nabla^2) \times \left\{ (N_m + N_e) \nabla^2 w - \rho h \frac{\partial^2 w}{\partial t^2} \right\} = 0 \tag{39}$$

where,

$$\nabla^4 = \frac{\partial^4}{\partial r^4} + \frac{2}{r} \frac{\partial^3}{\partial r^3} - \frac{1}{r^2} \frac{\partial^2}{\partial r^2} + \frac{1}{r^3} \frac{\partial}{\partial r} \tag{40}$$

According to Galerkin based reduced order model, deflection  $w(r,t)$  of the circular plate can be

approximated in terms of linear combinations of suitable shape functions with time dependent coefficients:

$$w(r,t) = \sum_{n=1}^{\infty} q_n(t) \psi_n(r), n=1,2,3,\dots \tag{41}$$

$$\psi_n(r) = J_0(\beta_n r) I_0(\beta_n R) - J_0(\beta_n R) I_0(\beta_n r) \tag{42}$$

where,  $\psi_n(r)$  are the natural vibration mode shapes of a circular plate and  $q_n(t)$  are the generalized time coordinates. The eigenvalues of fully clamped circular plates are given in Table 1.

Now, by substituting Equation (41) into Equation (39) the following equation is obtained:

$$\begin{aligned} &\tilde{c}_{11} \frac{h^3}{12} \sum_{n=1}^{\infty} \nabla^4 \psi_n(r) q_n(t) - (N_e + N_m) \sum_{n=1}^{\infty} \nabla^2 \psi_n(r) q_n(t) + \\ &\rho h \sum_{n=1}^{\infty} \psi_n(r) \ddot{q}_n(t) + (e_0 a)^2 (N_e + N_m) \sum_{n=1}^{\infty} \nabla^4 \psi_n(r) q_n(t) - \\ &\rho h (e_0 a)^2 \sum_{n=1}^{\infty} \nabla^2 \psi_n(r) \ddot{q}_n(t) = 0 \end{aligned} \tag{43}$$

According to Galerkin method, multiplying Equation (54) by  $r\psi_n(r)$ , integrating the result in domain  $r = [0, b]$  and using the orthogonality of Bessel functions, it yields as:

$$\begin{aligned} &[M]_{N \times N} \{\ddot{q}\}_{N \times 1} + [K]_{N \times N} \{q\}_{N \times 1} + [K_f]_{N \times N} + \\ &[K_f^{nl}]_{N \times N} \{q\}_{N \times 1} + [M^{nl}]_{N \times N} \{\ddot{q}\}_{N \times 1} = 0 \end{aligned} \tag{44}$$

where,

$$\begin{aligned} M(n,n) &= \rho h \int_0^R r \psi_n^2(r) dr, K(n,n) = \tilde{c}_{11} \frac{h^3}{12} \int_0^R \psi_n(r) \nabla^4 \psi_n(r) r dr, \\ K_f(n,n) &= -(N_m + N_e) \int_0^R \psi_n(r) \nabla^2 \psi_n(r) r dr, K_f^{nl}(n,n) = (e_0 a)^2 \times \\ &(N_m + N_e) \int_0^R \psi_n(r) \nabla^4 \psi_n(r) r dr, \\ M^{nl}(n,n) &= -\rho h (e_0 a)^2 \int_0^R \psi_n(r) \nabla^2 \psi_n(r) r dr \end{aligned} \tag{45}$$

In conclusion, the eigen matrix form of the governing equation is:

$$[M + M^{nl}] \{\ddot{q}\} + [K + K_f + K_f^{nl}] \{q\} = 0 \tag{46}$$

### 3. NUMERICAL RESULTS AND DISCUSSIONS

For numerical investigation of the problem, a fully clamped circular nano-plate with geometrical properties defined by  $R=10$  nm and  $h=0.335$  nm is considered. It is assumed that the nano-plate is constructed from the two-phase  $BaTiO_3-CoFe_2O_4$  composite material. Characteristics of the mentioned material for different

values of the volume fraction (V.F.) of piezoelectric phase are given in Table 2.

**TABLE 1.** Radial eigenvalues of clamped circular plate

m, n	1	2	3	4	5	6
$\beta_n R$	3.196	6.306	9.434	12.587	15.740	18.843

**TABLE 2.** Properties of BaTiO<sub>3</sub>- CoFe<sub>2</sub>O<sub>4</sub> composite material [22]

Type	1	2	3	4	5
V.F.	0%	25%	50%	75%	100%
C <sub>11</sub>	286	245	213	187	166
C <sub>12</sub>	173	139	113	93	77
C <sub>13</sub>	170	138	113	93.8	78
C <sub>33</sub>	269.5	235	207	183	162
C <sub>44</sub>	45.3	47.6	49.9	52.1	43
e <sub>31</sub>	0	-1.53	-2.71	-3.64	-4.4
e <sub>33</sub>	0	4.28	8.86	13.66	18.6
e <sub>15</sub>	0	0.05	0.15	0.46	11.6
k <sub>11</sub>	0.08	0.13	0.24	0.53	11.2
k <sub>33</sub>	0.093	3.24	6.37	9.49	12.6
$\mu_{11}$	5.9	3.57	2.01	0.89	0.05
$\mu_{33}$	1.57	1.21	0.839	0.47	0.1
q <sub>31</sub>	580	378	222	100	0
q <sub>33</sub>	700	476	292	136	0
d <sub>11</sub>	0	-3.09	-5.23	-6.72	0
d <sub>33</sub>	0	2334.15	2750	1847.49	0
$\rho$	5300	5430	5550	5660	5800

Unit: elastic constants,  $c_{ij}$ , in  $10^9$  N/m<sup>2</sup>, piezoelectric constants,  $e_{ij}$ , in C/m<sup>2</sup>, piezomagnetic constants,  $f_{ij}$ , in N/Am<sup>2</sup>, dielectric constants,  $k_{ij}$ , in  $10^{-9}$  c<sup>2</sup>/Nm<sup>2</sup>, magnetic constants,  $\mu_{ij}$ , in  $10^{-4}$  Ns<sup>2</sup>/c<sup>2</sup>, magneto-electric coefficients,  $d_{ij}$ , in  $10^{-12}$  Ns/Vc and density,  $\rho$ , in Kg/m<sup>3</sup>.

When magnetic and electric potentials are applied to the nano-plate, the axial compressive and tensile forces will be generated in the system, in which the axial compressive force may cause the instabilities. Axial compressive force is generated by applying positive electric or negative magnetic potential. It should be mentioned that imaginary part of eigenvalue is the natural frequency of the system. In instability point (divergence), fundamental natural frequency of the system tends to be zero. In Figures 2 and 3, the variation of imaginary parts of first two eigenvalues with applied electric and magnetic potentials is shown for third type

MEE nano-plate. These figures also show the points where the fundamental natural frequency becomes zero and therefore instability takes place. Critical values of magnetic and electric potentials for different types of MEE nano-plates considering various nonlocal parameters are calculated and presented in Tables 3 and 4.

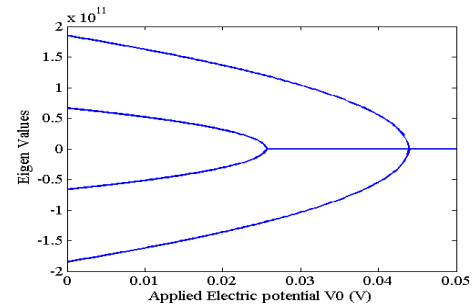


**Figure 2.** Divergence instability of third type nano-plate under electric potential  $V_0$ , with  $e_0a=2$  nm and  $\Omega_0=0$ .

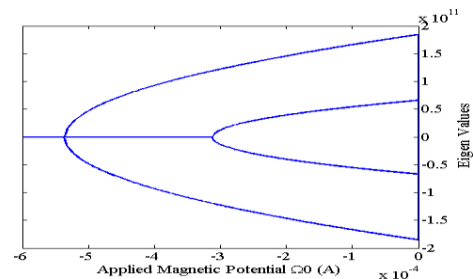


**Figure 3.** Divergence instability of third type nano-plate under magnetic potential  $\Omega_0$ , with  $e_0a=2$  nm and  $V_0=0$ .

**TABLE 3.** Calculated critical magnetic potentials for different volume fractions, with  $V_0=0$

$e_0a$	V.F.= 0%	V.F.= 25%	V.F.= 50%	V.F.= 75%
0.5	-0.00026	-0.0003425	-0.000505	-0.00099
1	-0.00023	-0.0003025	-0.00045	-0.0008775
1.5	-0.000195	-0.000255	-0.0003775	-0.00074
2	-0.00016	-0.00021	-0.00031	-0.0006075

**TABLE 4.** Calculated critical electric potentials for different volume fractions, with  $\Omega_0=0$

$e_0a$	V.F.= 25%	V.F.= 50%	V.F.= 75%	V.F.= 100%
0.5	0.08475	0.0415	0.027	0.01975
1	0.07525	0.0365	0.024	0.01775
1.5	0.06325	0.031	0.0205	0.01475
2	0.052	0.0255	0.0165	0.01225

Figure 4 shows the first six natural frequencies of the MEE circular nano-plate with 50 % volume fraction of BaTiO<sub>3</sub>, when different values of the nonlocal parameter are considered. The external magnetic and electric potentials are set as zero ( $V_0 = \Omega_0 = 0$ ). It is observed that for higher/lower values of nonlocal parameters the natural frequencies of the system are decreased/increased. From the data of this figure, it can be clarify that, as the mode number increases, the influence of size effect on natural frequencies increases. It is indicated that size dependence of the material properties decreases the stiffness of the nano-plate and hence decreases the values of frequencies.

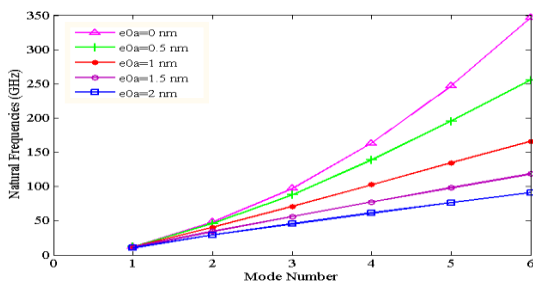


**Figure 4.** First six natural frequencies of the third type MEE circular nanoplate for various values of  $e_0a$ , with  $V_0 = \Omega_0 = 0$ .

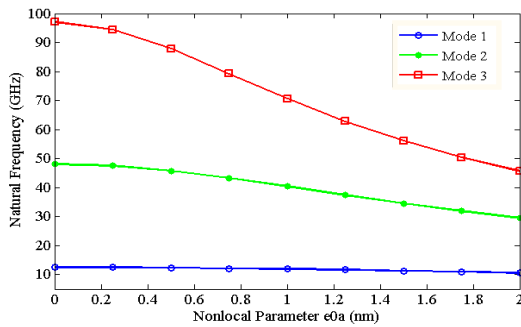


**Figure 5.** Effect of nonlocal parameter on the third type MEE nano-plate's natural frequencies for different mode numbers ( $V_0 = \Omega_0 = 0$ ).

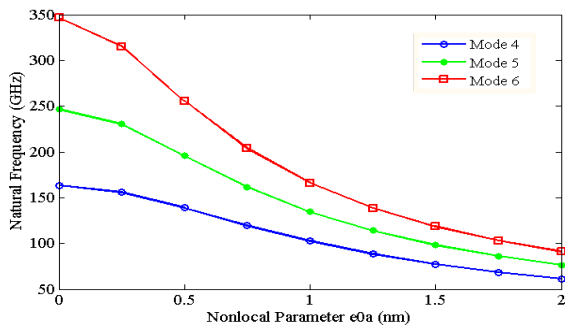


**Figure 6.** Effect of nonlocal parameter on the third type MEE nano-plate's natural frequencies for different mode numbers ( $V_0 = \Omega_0 = 0$ ).

The variations of the first six natural frequencies of the nano-plate versus the nonlocal parameter for various mode numbers are indicated in Figures 5 and 6. As expected, the natural frequencies decrease with an increase in the nonlocal parameter. Obviously, as the nonlocal parameter increases, the natural frequencies of different modes converge to each other.

The variations of the first natural frequency of the nano-plate versus the radius of the nano-plate, for different values of the nonlocal parameters are plotted in Figure 7. It is considered the radius of the nano-plate to be changing from 5 to 14 nm. Because of decreasing in stiffness of the plate, it is obvious that the natural frequencies of the system decrease with the increase of the radius. Besides, one can understand from these figures that the decrease rate of the natural frequencies is more considerable in smaller radius. Consequently, it can be easily concluded that for the bigger radius values, the effect of nonlocal parameter on the natural frequency will be vanished and is negligible. In other words, for larger enough values of the radius, there is not seen any difference between the classical and nonclassical nonlocal theories. When the radius of the nano-plate exceeds a specified value, the natural frequencies decrease by the same rate. Furthermore, it is clear that for larger values of the radius, the effects of the nonlocal parameter on the natural frequency decrease. Changing of the first natural frequency of the nano-plate with the volume fraction of the BaTiO<sub>3</sub> phase in the MEE composite material is depicted in Figure 8, when various values of the nonlocal parameters are applied. The volume fraction changes from 0 to 100 %. When the volume fraction is 0 %, the composite material is pure piezomagnetic and when the volume fraction is 100 %, the composite material is pure piezoelectric material. The data would seem to suggest that, the natural frequencies of the nano-plate decrease while the volume fraction rises from 0 to 100 %. The reason is that by increasing the volume fraction in the MEE material, the effective Young's modulus of the nano-plate decreases.

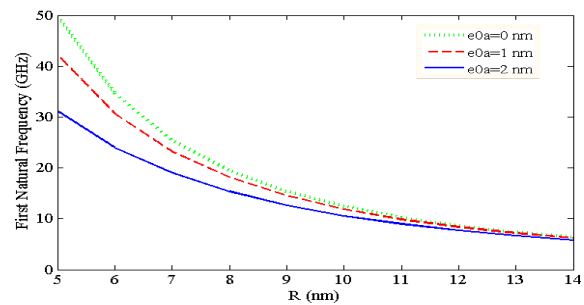


**Figure 7.** Variations of the first natural frequency versus the radius value of the third type MEE nano-plate ( $h=0.335$  nm), for different values of nonlocal parameter.

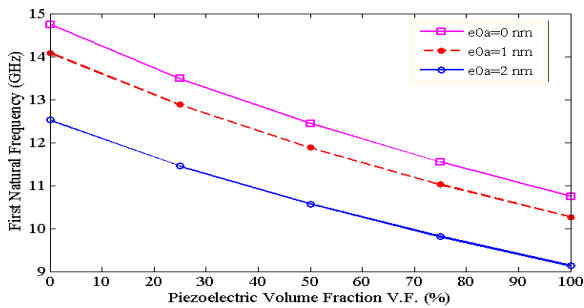


**Figure 8.** Variations of the first natural frequency of the MEE nano-plate with the volume fraction of piezoelectric phase, for different values of the nonlocal parameters.

Decreasing of the effective Young’s modulus makes the stiffness of the nano-plate to decrease. Therefore, the natural frequencies of the nano-plate decrease.

Figure 9 plots first natural frequency for nano-plate as a function of thickness for given values of nonlocality when no external magnetic and electric potentials are applied. The thickness of the nano-plate is taken to be in the range between of 0.2 to 1 nm. The most prominent result can be seen from this figure is that the natural frequencies increase linearly with the increase of thickness of the nano-plate. Second, as the nonlocal parameter increases, the slope of the diagrams decreases. Third, the natural frequencies predicted by the present non-classical fully clamped plate model are always lower than those by classical plate model. Besides, the increase of the plate thickness can lead to the increase the difference between classic and nonclassic nonlocal theories. The effects of the external electric potential  $V_0$  on the natural frequencies of the first three modes of the nano-plate is presented in Figure 10. The MEE nano-plate is constructed from 50 % volume fraction of BaTiO<sub>3</sub>. The nonlocal parameter is set to be 2 nm. The applied electric potential changes from -0.009 to 0.009 volt.

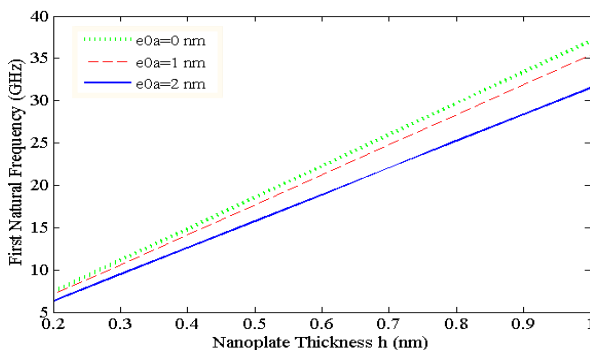


**Figure 9.** The effect of the thickness  $h$  on the first natural frequency of the third type MEE nano-plate with  $R= 10$  nm,  $V_0= \Omega_0=0$ .

It is clear that the electric potential has a considerable effect on the natural frequencies of the MEE nano-plates.

This figure reveals that the natural frequencies of the MEE nano-plate decrease when the electric potential  $V_0$  increases. The reason of this phenomenon is that when a negative/positive electric potential is applied to the system, the tension/compressive radial forces are generated in the nano-plate. These forces influence the stiffness of the nano-plates. For example, when the positive electric potential increases, the generated compressive force increases and therefore the stiffness and consequently natural frequencies of the nano-plate decrease. The diagram of the variations of the first three natural frequencies of the third type of MEE circular nano-plate with external magnetic potential  $\Omega_0$ , considering nonlocal parameter equal 2 nm, is plotted in Figure 11. The applied magnetic potential is taken to be in the range of -0.09 to 0.09 mA. It is obvious that the natural frequencies are considerably influenced by the external magnetic potential. One can understand from this figure that increasing of the external magnetic potential reduces the natural frequencies of the nano-plate. This is due to this fact that compressive and tension radial forces are generated respectively when negative and positive magnetic potentials are applied to the nano-plate. Therefore, it can be concluded that the stiffness and consequently the natural frequencies of the MEE nano-plate are affected by the external magnetic potential.

Figure 12 plots variation of first natural frequency with respect to applied electric potential for several values of nonlocal factor. A prominent result found here is that the decreasing rate of the natural frequency versus the electric potential increases when the nonlocal parameter is set to be larger. Figure 13 indicates variation of first natural frequency with applied magnetic potential for various values of nonlocal parameter.

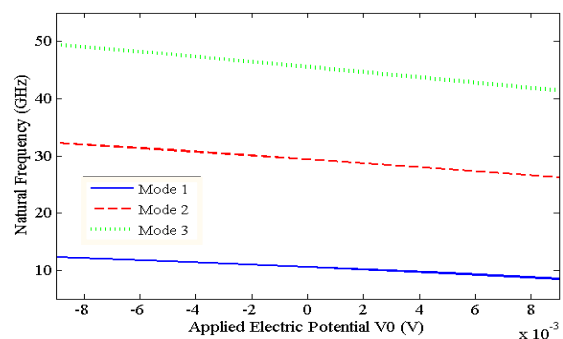


**Figure 10.** The effect of the applied external electric potential  $V_0$  on the natural frequencies of the third type MEE nano-plate with  $\Omega_0=0$  and  $e_0a= 2$  nm.

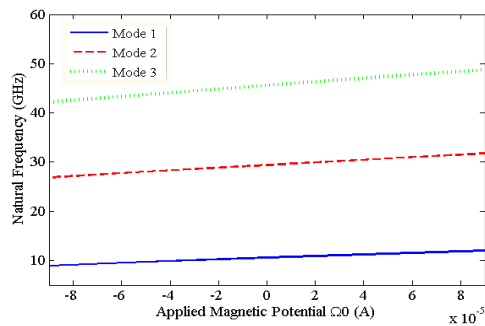


**Figure 11.** The effect of the applied external magnetic potential  $\Omega_0$  on the natural frequencies of the third type MEE nano-plate with  $V_0=0$  and  $e_0a=2$  nm.

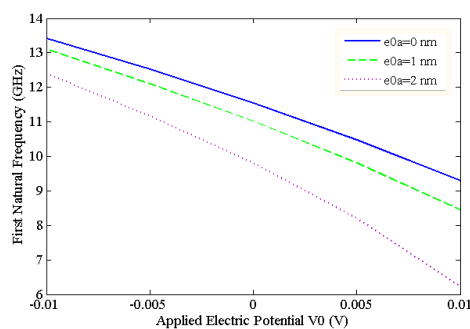


**Figure 12.** The effect of the applied external electric potential  $V_0$  on the first natural frequency of the fourth type MEE nano-plate with  $\Omega_0=0$ , for different values of nonlocal parameter  $e_0a$ .

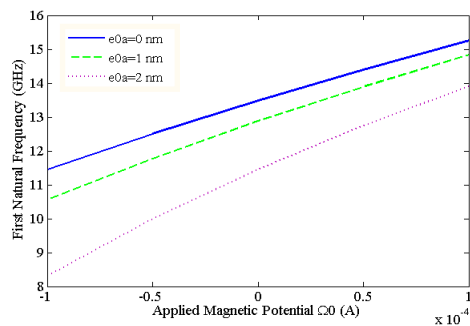


**Figure 13.** The effect of the applied external magnetic potential  $\Omega_0$  on the first natural frequency of the second type MEE nano-plate with  $V_0=0$ , for different values of nonlocal parameter  $e_0a$ .

Similarly, it is seen that for higher values of nonlocal parameter, the increasing rate of the natural frequency with magnetic potential increases. At last, as can be observed from Figures 12 and 13, the difference between classic and size-dependent natural frequencies decreases by decreasing /increasing of the applied electric/magnetic potential. In other words, large enough

tensional force leads the diagrams converge to each other.

#### 4. CONCLUDING REMARKS

Coming to conclusion, this study set out in order to investigate the size-dependent free vibration of a circular fully clamped MEE nano-plate under external magnetic and electric potentials using Kirchhoff's plate theory based on Eringen's nonlocal elasticity. Nonlocal constitutive relations for MEE materials, Maxwell's equation and Hamilton's principle were used to derive the governing equation of the nano-plate. Using Galerkin approach, the obtained equation was transformed to an eigen matrix form and subsequently was solved numerically to find the natural frequencies. From numerical results, the following conclusions were obtained. Increasing the nonlocal parameter caused the natural frequencies to decrease. For larger values of nonlocal parameter, the influence of mode number on the natural frequencies decreased. When the radius value of the nano-plate exceeded a specific value, the effect of the nonlocal parameter vanished. Increasing of the piezoelectric phase's volume fraction brings reduction in the natural frequencies. In thick nano-plates compared to the thin ones, effect of the nonlocal parameter was more considerable. Furthermore, increasing rate of the natural frequencies with the increase of thickness value was lower for the higher values of nonlocal parameter. Sensitivity of MEE circular nano-plates to the magneto-electric loadings was more considerable in which the results showed that the natural frequencies decrease with the increase of the applied electric potential. In contrast, the numerical calculation demonstrated that the applying magnetic potential has an increasing effect on the natural frequencies. Difference between classic and nonclassical natural frequencies increased/decreased with the increase of electric/magnetic potential. Decreasing/increasing rate of the natural frequencies with the electric/magnetic potential was higher for larger values of nonlocal parameter.

#### 5. REFERENCES

1. Farajpour, A., Mohammadi, M., Shahidi, A.R. and Mahzoon, M., "Axisymmetric buckling of the circular graphene sheets with the nonlocal continuum plate model", *Physica E*, Vol. 43,(2011),1820-1825.
2. Shah-Mohammadi-Azar, A., Khanchehgardan, A., Rezazadeh, G. and Shabani, R., "Mechanical response of a piezoelectrically sandwiched nano-beam based on the nonlocal theory", *International Journal of Engineering-Transactions C: Aspects*, Vol. 26, No. 12, (2013), 1515-1524.



3. Shabani, R., Sharafkhani, N. and Gharebagh, V.M., "Static and dynamic response of carbon nanotube-based nano-tweezers", *International Journal of Engineering-Transactions A: Basics*, Vol. 24, No. 4, (2011), 377-385.
4. Malekzadeh, P. and Shojaee, M., "Free vibration of nanoplates based on a nonlocal two-variable refined plate theory", *Composite Structures*, Vol.95,(2013), 443-453.
5. Khanchehgardan, A., Shah-Mohammadi Azar, A., Rezazadeh, G. and Shabani, R., "Thermo-elastic damping in nano-beam resonators based on nonlocal theory", *International Journal of Engineering-Transactions C: Aspects*, Vol. 26, No. 12, (2013), 1505-1514.
6. JafarSadeghi-Pournaki, I., Zamanzadeh, M.R., Madinei, H. and Rezazadeh, G., "Static pull-in analysis of capacitive FGM nanocantilevers subjected to thermal moment using Eringen's nonlocal elasticity", *International Journal of Engineering-Transactions A: Basics*, Vol. 27, No. 4, (2014), 633-642.
7. Liu, C., Ke, L.L., Wang, Y.S., Yang, J. and Kitipornchai, S., "Thermo-electro-mechanical vibration of piezoelectric nanoplates based on the nonlocal theory", *Composite Structures*, Vol. 106, (2013),167-174.
8. Farajpour, A., Dehnaghy, M. and Shahidi, A.R., "Surface and nonlocal effects on the axisymmetric buckling of circular graphene sheets in thermal environment", *Composites Part B: Engineering*, Vol. 50, (2013), 333-343.
9. Cheng, C.H. and Chen, T., "Size-dependent resonance and buckling behavior of nanoplates with High-order surface stress effects", *Physica E*, Vol. 67, (2015), 12-17.
10. Zhou, Z.G., Wang, B. and Sun, Y.G., "Two collinear interface cracks in magneto-electro-elastic composites", *International Journal of Engineering Science*, Vol. 42, (2004), 1155-1167.
11. Li, J.Y., "Magneto-electro-elastic multi-inclusion and inhomogeneity problems and their applications in composite materials", *International Journal of Engineering Science*, Vol. 38, (2000), 1993-2011.
12. Pan, E. and Heyliger, P.R., "Exact solutions for magneto-electro-elastic laminates in cylindrical bending", *International Journal of Solids and Structures*, Vol. 40, (2003), 6859-6876.
13. Pakam, N. and Arockiarajan, A., "Study on effective properties of 1-3-2 type magneto-electro-elastic composites", *Sensors and Actuators A: Physical*, Vol. 209, (2014), 87-99.
14. Giordano, S., "Explicit nonlinear homogenization for magneto-electro-elastic laminated materials", *Mechanics Research Communications*, Vol. 55, (2014), 18-29.
15. Chang, T.P., "On the natural frequency of transversely isotropic magneto-electro-elastic plates in contact with fluid", *Applied Mathematical Modelling*, Vol. 37, (2013), 2503-2515.
16. Li, Y.S., "Buckling analysis of magneto-electro-elastic plate resting on Pasternak elastic foundation", *Mechanics Research Communications*, Vol. 56, (2014), 104-114.
17. Alaimo, A., Milazzo, A. and Orlando, C., "A four-node MITC finite element for magneto-electro-elastic multilayered plates", *Composite Structures*, Vol. 129, (2013), 120-133.
18. Chang, T.P., "Deterministic and random vibration analysis of fluid-contacting transversely isotropic magneto-electro-elastic plates", *Computers & Fluids*, Vol. 84, (2013), 247-254.
19. Liu, M.F., "An exact deformation analysis for the magneto-electro-elastic fiber-reinforced thin plate", *Applied Mathematical Modelling*, Vol. 35, (2011), 2443-2461.
20. Xue, C.X., Pan, E., Zhang, S.Y. and Chu, H.J., "Large deflection of a rectangular magneto-electro-elastic thin plate", *Mechanics Research Communications*, Vol. 38, (2011), 518-523.
21. Li, Y.S., Cai, Z.Y. and Shi, S.Y., "Buckling and free vibration of magneto-electro-elastic nanoplate based on nonlocal theory", *Composite Structures*, Vol. 111, (2014), 522-529.
22. Xue, C.X. and Pan, E., "On the longitudinal wave along a functionally graded magneto-electro-elastic rod", *International Journal of Engineering Science*, Vol. 62, (2013), 48-55.
23. Ke, L.L. and Wang, Y.S., "Free vibration of size-dependent magneto-electro-elastic nanobeams based on the nonlocal theory", *Physica E*, Vol. 63, (2014), 52-61.
24. Chan, K. and Zhao, Y., "The dispersion characteristics of the waves propagating in a spinning single-walled carbon nanotube", *Science China Physics, Mechanics and Astronomy*, Vol. 54, No. (10), (2011), 1854-1865.

# Vibration Analysis of Circular Magneto-Electro-Elastic Nano-plates Based on Eringen's Nonlocal Theory

A. Amiri, S. M. Fakhari, I. J. Pournaki, G. Rezazadeh, R. Shabani

Department of Mechanical Engineering, Urmia University, Urmia, Iran

---

## PAPER INFO

چکیده

---

### Paper history:

Received 16 October 2015

Received in revised form 15 November 2015

Accepted 24 December 2015

---

### Keywords:

Magneto-electro-elastic

Nano-plates

Kirchhoff's Plate Theory

Nonlocal Elasticity

Natural Frequency

در این مقاله ارتعاشات آزاد نانو صفحات مدور مگنتو-الکترو-الاستیک، با استفاده از تئوری الاستیسیته غیرموضعی و بر اساس فرضیه تئوری صفحه کیرشهف مطالعه می شود. نانوصفحه مورد مطالعه به صورت کامل گیردار بوده و در معرض پتانسیل های مغناطیسی و الکتریکی خارجی می باشد. با در نظر گرفتن روابط بنیادی غیر موضعی حاکم بر مواد مگنتو-الکترو-الاستیک و با اعمال معادله ماکسول و اصل همیلتون، معادلات حاکم به دست آمده است. با به کار گیری روش گلرکین، فرم ماتریسی معادله حاکم به دست می آید. اثر پتانسیل مغناطیسی-الکتریکی بر ناپایداری سیستم بررسی می گردد و به تبع آن مقادیر بحرانی پتانسیل های اعمالی به دست می آیند. اثرهای اندازه، ضخامت و شعاع نانو صفحه و درصد حجمی فاز پیزوالکتریک بر فرکانس های طبیعی نانوصفحه به صورت تفصیلی مطالعه شده است. به علاوه اثرهای پتانسیل های مغناطیسی و الکتریکی بر فرکانس های طبیعی وابسته به اندازه مورد بررسی قرار می گیرد.

**doi:**10.5829/idosi.ije.2015.28.12c.15

---